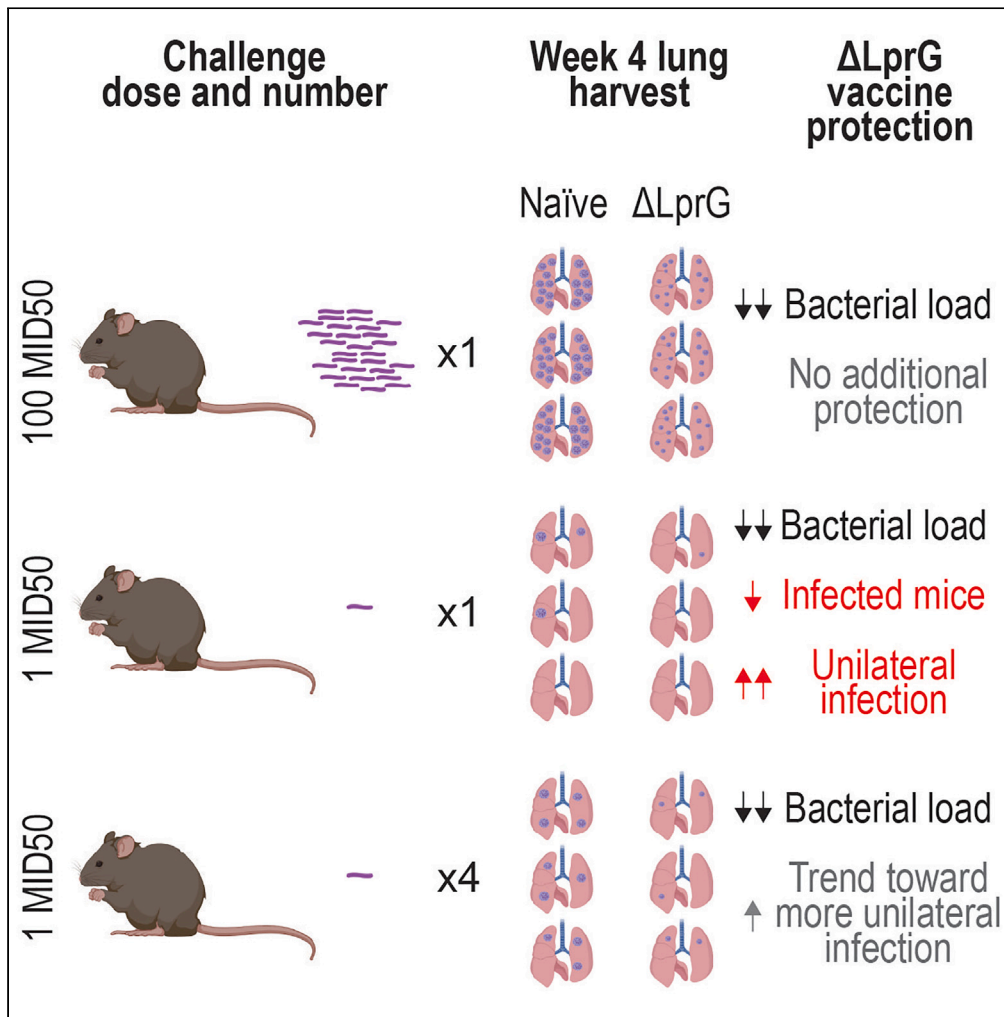**Article**

Attenuated *Mycobacterium tuberculosis* vaccine protection in a low-dose murine challenge model

Samuel J. Vidal,
Daniel Sellers,
Jingyou Yu, ...,
Kevin B. Urdahl,
Amanda J.
Martinot, Dan H.
Barouch

dbarouch@bidmc.harvard.edu

Highlights

ΔLprG reduces detectable
infection in mice after
single 1 MID50 challenge

ΔLprG prevents infection
dissemination after single
1 MID50 challenge

Repeated 1 MID50
challenge facilitates
correlates of ΔLprG
vaccine protection

Article

Attenuated *Mycobacterium tuberculosis* vaccine protection in a low-dose murine challenge model

Samuel J. Vidal,[1,2] Daniel Sellers,[1] Jingyou Yu,[1] Shoko Wakabayashi,[3] Jaimie Sixsmith,[3] Malika Aid,[1] Julia Barrett,[1] Sage F. Stevens,[1] Xiaowen Liu,[4] Wenjun Li,[5] Courtney R. Plumlee,[6] Kevin B. Urdahl,[6,7,8] Amanda J. Martinot,[9] and Dan H. Barouch[1,10,11,*]

SUMMARY

Bacillus Calmette–Guérin (BCG) remains the only approved tuberculosis (TB) vaccine despite limited efficacy. Preclinical studies of next-generation TB vaccines typically use a murine aerosol model with a supraphysiologic challenge dose. Here, we show that the protective efficacy of a live attenuated *Mycobacterium tuberculosis* (Mtb) vaccine ΔLprG markedly exceeds that of BCG in a low-dose murine aerosol challenge model. BCG reduced bacterial loads but did not prevent establishment or dissemination of infection in this model. In contrast, ΔLprG prevented detectable infection in 61% of mice and resulted in anatomic containment of 100% breakthrough infections to a single lung. Protection was partially abrogated in a repeated low-dose challenge model, which showed serum IL-17A, IL-6, CXCL2, CCL2, IFN-γ, and CXCL1 as correlates of protection. These data demonstrate that ΔLprG provides increased protection compared to BCG, including reduced detectable infection and anatomic containment, in a low-dose murine challenge model.

INTRODUCTION

Tuberculosis (TB) is a leading cause of mortality from infectious disease worldwide with more than 1.5 million deaths in 2020.[1] Bacillus Calmette–Guérin (BCG) demonstrates high efficacy against disseminated infection in children, but lifetime efficacy in adults ranges widely between 0% and 80%.[2] Despite this limited efficacy, BCG has remained the sole clinically approved vaccine for nearly a century.[3] Accordingly, the development of next-generation vaccines with favorable safety and improved efficacy profiles relative to BCG is an urgent global health priority.[4] We recently developed a live attenuated vaccine derived from the virulent *Mycobacterium tuberculosis* (Mtb) H37Rv strain termed ΔLprG with a deletion in *rv1411c-rv1410c*, an operon that encodes a lipoprotein (LprG) and transmembrane efflux pump (Rv1410) that function as a lipid transporter whose disruption results in altered lipid content of the Mtb cell wall as well as its metabolic state.[5] ΔLprG was well tolerated in immunocompromised mice and demonstrated greater immunogenicity and reductions in bacterial burdens than BCG after 100 colony-forming unit (CFU) aerosol challenge.[5,6]

The murine challenge model has proved valuable for studying TB pathophysiology and vaccine development. For example, the essential contributions of CD4 T cells[7] interferon gamma (IFN-γ)[8,9] and tumor necrosis factor alpha (TNF-α)[10] were described in mice. Furthermore, the antigens comprising the M72/AS01$_E$ TB vaccine candidate were characterized in mice.[11,12] However, Mtb is likely transmitted by small respiratory droplets containing few bacilli,[13,14] and the widely employed 100 CFU murine aerosol challenge model generally fails to recapitulate key hallmarks of human disease including granulomatous inflammation[15] and heterogeneous infections.[16] Moreover, the protective efficacy of vaccines is limited to moderate reductions in bacterial burdens, complicating the preclinical interpretation of results in this model. Accordingly, the development of preclinical models that are both experimentally tractable and more reminiscent of human disease is important for next-generation vaccine development.[17]

Recently, a lower dose 1–3 CFU murine aerosol model showed heterogeneous bacterial loads as well as a subset of mice with unilateral infection, and barcoding experiments showed that most cases of bilateral infection were driven by dissemination of a single infecting bacterium to the contralateral lung.[18] Moreover, additional studies in this model found that BCG immunization improved long-term control of

[1]Center for Virology and Vaccine Research, Beth Israel Deaconess Medical Center, Harvard Medical School, Boston, MA, USA

[2]Division of Infectious Diseases, Brigham and Women's Hospital, Harvard Medical School, Boston, MA, USA

[3]Department of Immunology and Infectious Diseases, Harvard T.H. Chan School of Public Health, Boston, MA, USA

[4]Department of Emergency Medicine, Beth Israel Deaconess Medical Center, Boston, MA, USA

[5]Department of Public Health, University of Massachusetts Lowell, Lowell, MA, USA

[6]Center for Global Infectious Disease Research, Seattle Children's Research Institute, Seattle, WA, USA

[7]Department of Pediatrics, University of Washington, Seattle, WA, USA

[8]Department of Immunology, University of Washington, Seattle, WA, USA

[9]Department of Infectious Diseases and Global Health, Tufts University Cummings School of Veterinary Medicine, North Grafton, MA, USA

[10]Ragon Institute of MGH, MIT and Harvard, Cambridge, MA, USA

[11]Lead contact

*Correspondence: dbarouch@bidmc.harvard.edu

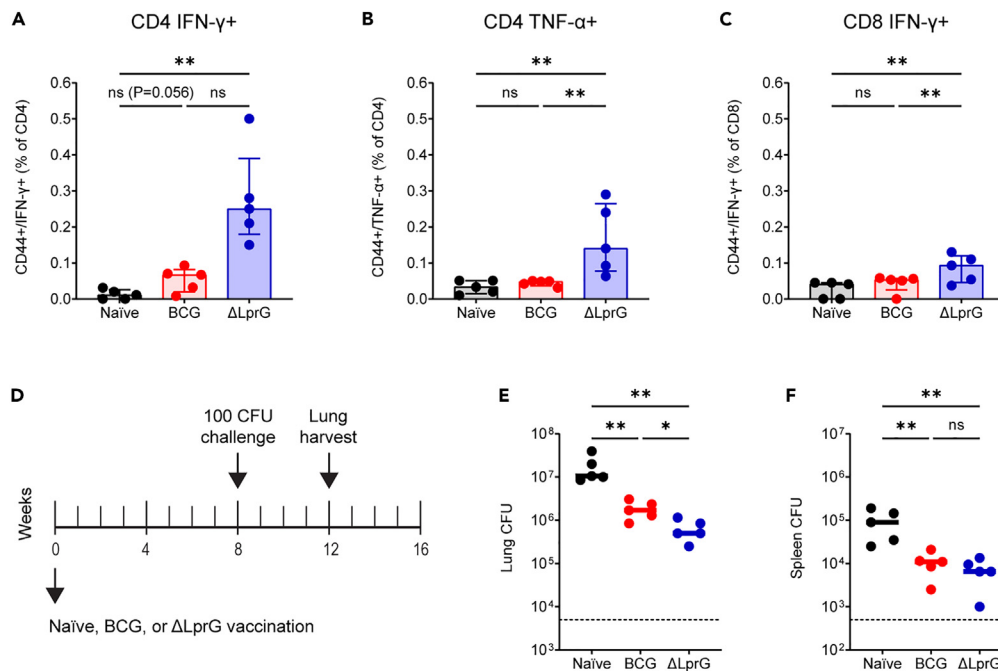https://doi.org/10.1016/j.isci.2023.106963

Figure 1. ΔLprG is more immunogenic and protective than BCG following 100 CFU H37Rv challenge in C3HeB/FeJ mice

(A–C) Groups of C3HeB/FeJ mice were immunized with BCG (n = 5) or ΔLprG (n = 5) at week 0 followed by PBMC ICS following stimulation with purified protein derivative (PPD) at week 2 to quantify subsets including CD4 IFN-γ+ T cells (A), CD4 TNF-α+ T cells (B), and CD8 IFN-γ+ T cells (C).

(D) Challenge study design (D).

(E) Groups of C3HeB/FeJ mice were immunized with BCG (n = 5) or ΔLprG (n = 5) at week 0 followed by 100 CFU H37Rv aerosol challenge at week 8 and lung and spleen harvesting at week 12 for bacterial load quantification. Lung CFU from the challenge study (E).

(E) Bottom dotted line represents assay LOD of 5,000 CFU. Spleen CFU from the challenge study (F). Bottom dotted line represents assay LOD of 500 CFU. For (A)–(C), data are represented as median +/− interquartile range. For (E) and (F), bars represent group medians. For all panels, p values represent pairwise Mann Whitney U tests. For all panels, * represents p < 0.05 and ** represents p < 0.01.

bacterial loads, prevented dissemination of barcoded bacilli to contralateral lung, and reduced the proportion of mice with detectable infection, although these studies required large numbers of mice due to the low protective efficacy of BCG.[19,20] In this study, we evaluated the protective efficacy of BCG and the more potent live attenuated ΔLprG vaccine candidate in the low-dose model.[5,6] Compared to BCG, ΔLprG yielded protection from detectable infection in a substantial subset of mice and anatomic containment in all animals with breakthrough infection.

RESULTS

ΔLprG is immunogenic and protective after 100 CFU challenge

We first sought to confirm the immunogenicity and protective efficacy of the live attenuated ΔLprG vaccine strain against a 100 CFU challenge. We focused these studies in C3HeB/FeJ mice, which exhibit susceptibility to Mtb infection and show granulomas with central caseous necrosis that are reminiscent of human disease.[21] Mice were vaccinated at week 0 with BCG or ΔLprG, and we measured purified protein derivative-specific T cell responses in peripheral blood mononuclear cells (PBMCs) at week 2 by intracellular cytokine staining. BCG did not elicit significant CD4 IFN-γ-secreting (Figure 1A), CD4 TNF-α-secreting (Figure 1B), or CD8 IFN-γ-secreting (Figure 1C) responses in PBMCs at this time point. In contrast, ΔLprG stimulated significant cytokine-secreting T cells responses of all three phenotypes (Figures 1A–1C). CD4 IL-2 responses were not detected as previously reported.[5] Next, we performed multiplexed serum cytokine analysis in naive and vaccinated mice at week 2.5. Compared to naive mice, BCG-vaccinated mice showed upregulation of serum cytokines including IFN-γ, TNF-α, and interleukin-17A (IL-17A), among others (Figures S1A and S1B). ΔLprG also
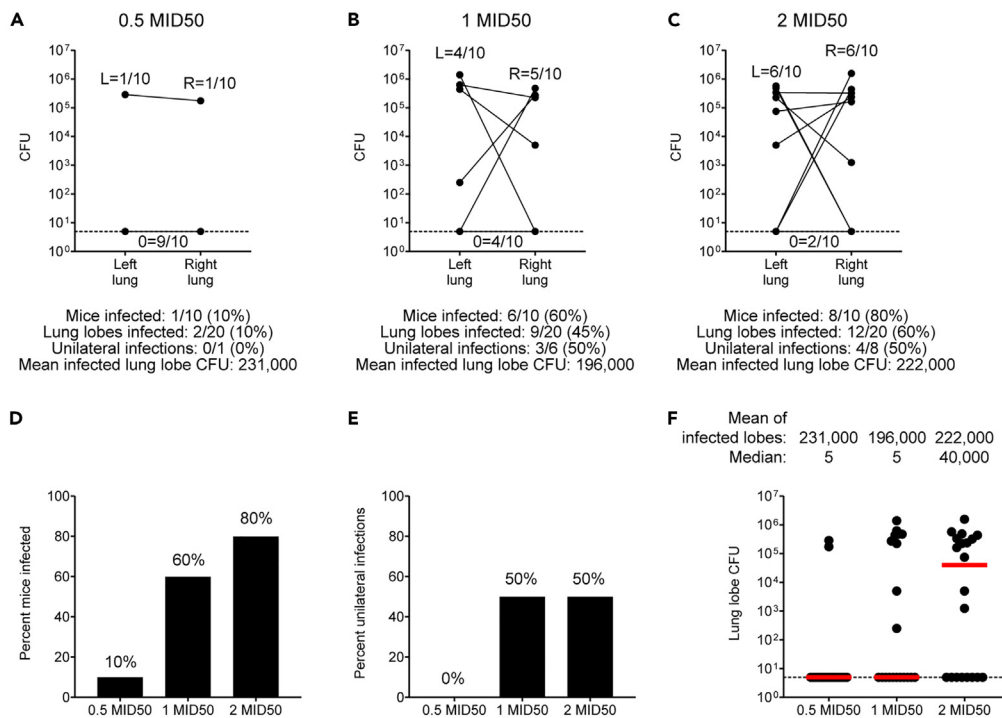
Figure 2. Characterization of 1 MID50 H37Rv challenge in C3HeB/FeJ mice

(A–C) Single-cell suspension H37Rv challenge stock $\log_2$-scale *in vivo* dose-finding study (A–C). C3HeB/FeJ mice (n = 10 per group) were challenged at week 0 with the indicated challenge stock doses followed by right and left lung lobe harvesting at week 4 for bacterial load quantification. Bottom dotted line represents assay LOD of 5 CFU.

(D–F) Histograms and dot plots summarizing infection rates and bacterial loads shown in A–C (D–F). For (F), dotted bottom line represents assay LOD of 5 CFU and bars represent group medians.

stimulated upregulation of serum cytokines including IFN-γ, TNF-α, and IL-17A, among others (Figures S1A and S1B). There were no cytokines differentially detected between BCG and ΔLprG, although ΔLprG showed a trend toward greater IL-17A levels (Figure S1C) as previously reported.[5]

We next assessed the protective efficacy of BCG and ΔLprG against a 100 CFU H37Rv aerosol challenge. Groups of C3HeB/FeJ mice (n = 5 per group) were vaccinated at week 0 with BCG or ΔLprG, challenged at week 8 with 100 CFU of H37Rv by the aerosol route, and lungs and spleens were harvested at week 12 for bacterial load quantification. ΔLprG yielded a greater reduction in bacterial loads in the lung relative to BCG, as we previously reported,[5] and both vaccines reduced bacterial loads in the spleen (Figures 1E and 1F). Thus, ΔLprG showed a more favorable immunogenicity and protective efficacy profile against 100 CFU challenge.

Characterization of 1 MID50 challenge in C3HeB/FeJ mice

To adapt the low-dose challenge model, we first performed a $\log_{10}$ *in vivo* titration of a single-cell suspension H37Rv challenge stock to determine a dose that produced a 60%–70% infection rate[18] (data not shown). We next performed a more focused $\log_2$-scale *in vivo* dose-finding study, harvesting separately dissected right and left lung lobes 4 weeks after challenge of 30 C3HeB/FeJ mice (n = 10 mice per group) with the single-cell suspension H37Rv challenge stock. This study yielded infection rates of 10%, 60%, and 80% with a limit of detection (LOD) of 5 CFU per lung lobe (Figures 2A–2D). These studies demonstrated heterogeneous bacterial loads spanning an approximately 4 $\log_{10}$ range and showed that subsets of mice demonstrated unilateral infection with Mtb CFU detected solely in the right or left lung lobe (Figures 2E and 2F).

In order to formulate a quantitative nomenclature for challenge doses, and given that the intermediate challenge dose yielded a 60% infection rate (Figure 2B), we termed this challenge dose 1 median infectious dose 50 (1 MID50). We further calculated that the bacterial inoculum required for 100 CFU challenge was approximately 2 $\log_{10}$ higher than for the 1 MID50 challenge, and we therefore termed this challenge dose 100 MID50.
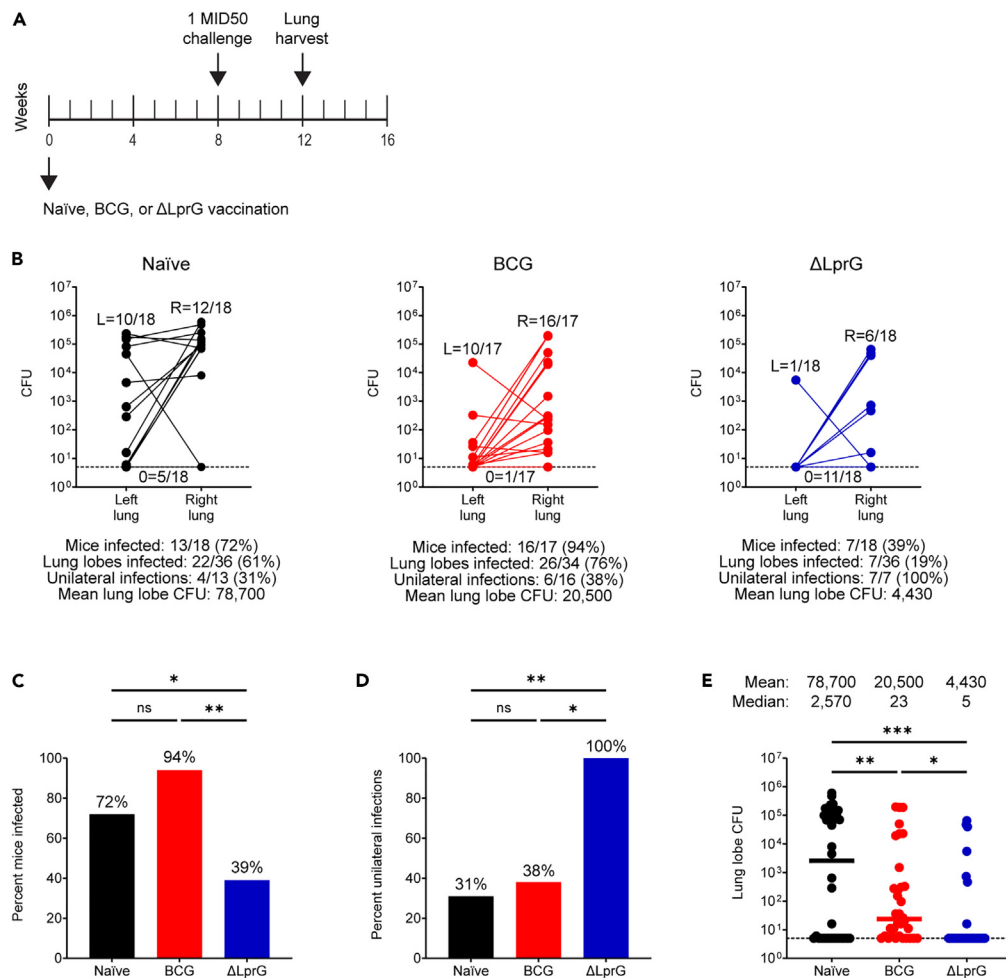
Figure 3. Vaccine protection with BCG and ΔLprG after 1 MID50 H37Rv challenge in C3HeB/FeJ mice
(A) Study design (A).
(B) Three cohorts of C3HeB/FeJ mice (n = 18 mice per cohort, n = 54 mice total) were divided equally into naive, BCG, and ΔLprG groups. Vaccines were administered at week 0 followed by 1 MID50 H37Rv aerosol challenge at week 8 and right and left lung lobe harvesting at week 12 for bacterial load quantification (B).
Bottom dotted line represents an LOD of 5 CFU. Histograms and dot plots summarizing data are shown in B (C–E). p values for infection rates between groups represent an exact logistic regression model (C and D). p values for bacterial loads between groups represent a mixed effects negative binomial model (E). For (E), dotted bottom line represents an LOD of 5 CFU and bars represent group medians. For all panels, * represents $p < 0.05$, ** represents $p < 0.01$, and *** represents $p < 0.001$.

Finally, we performed histopathological studies comparing the lung tissues of mice after either 1 MID50 or 100 MID50 H37Rv aerosol challenge. 1 MID50 mice showed fewer granulomas than 100 MID50 mice, and when identified granulomas were smaller and solitary in 1 MID50 compared to 100 MID50 mice (Figures S2A and S2D). In some cases, 1 MID 50 mice showed only rare foci of alveolitis characterized by increased numbers of alveolar macrophages and minimal expansion of the interstitium with lymphocytes and perivascular lymphocyte cuffing (Figures S2B and S2E). Acid-fast staining revealed multibacillary (>2 bacilli per macrophage) replication of Mtb in 100 MID50 mice compared to typically paucibacillary macrophage infection in 1 MID50 mice (Figures S2C and S2F).

ΔLprG reduces infection and dissemination after 1 MID50 challenge compared to BCG

We next performed vaccine studies with BCG and ΔLprG using 1 MID50 challenge (Figure 3A). Three cohorts of C3HeB/FeJ mice (n = 18 mice per cohort, n = 54 total mice) were divided equally into three groups including naive, BCG, and ΔLprG. Mice were vaccinated at week 0 and underwent a 1 MID50 H37Rv aerosol

challenge at week 8. At week 12, right and left lung lobes were dissected separately and bacterial loads were quantified with an LOD of 5 CFU. The pooled infection rate in the naive group was 13/18 (72%, Figure 3B), confirming reproducibility of achieving the challenge dose associated with 1 MID50 infection.[18] Among infected naive animals, there were 4/13 (31%) unilateral infections (Figure 3B). As before, we observed a broad distribution of bacterial loads with a mean lung lobe bacterial burden of 4.90 $\log_{10}$ CFU (Figure 3B).

In the BCG group, we observed an infection rate of 16/17 (95%) including a unilateral infection rate of 6/16 (38%, Figure 3B). We used an exact logistic regression model to compare both rates of mouse infection (in either one or both lungs) and rates of dissemination (among infected mice to both lungs) between vaccine groups. We observed no difference in the rate of infection or dissemination between the naive and BCG groups (p = 0.12 for both comparisons, exact logistic regression, Figures 3C and 3D). In addition, we used an ordinal logistic regression model to compare a composite outcome including both infection and dissemination between vaccine groups. We observed no difference in this composite outcome between the naive and BCG groups (p = 0.29, ordinal logistic regression). However, BCG did yield a 0.58 $\log_{10}$ reduction in mean lung lobe CFU relative to the naive group (p < 0.001, mixed effects negative binomial, Figure 3E). Thus, BCG reduced bacterial burdens but failed to abort establishment or dissemination of infection after 1 MID50 challenge.

In contrast to BCG, ΔLprG yielded an infection rate of 7/18 (39%), and all breakthrough mice (7/7, 100%) demonstrated unilateral infection (Figure 3B). The infection rate in the ΔLprG group was lower compared to both the naive and BCG groups (p = 0.049 and p = 0.005, respectively, exact logistic regression, Figure 3C), and the unilateral infection rate was higher compared to both the naive and BCG groups (p = 0.009 and p = 0.014, respectively, exact logistic regression, Figure 3D). Moreover, the composite outcome of infection and dissemination was lower in the ΔLprG group compared to both the naive and BCG groups (p = 0.002 and p = 0.001, respectively, ordinal logistic regression). Finally, the ΔLprG group showed a 1.3 $\log_{10}$ reduction in mean lung lobe CFU relative to the naive group, which also represented a 0.67 $\log_{10}$ reduction relative to the BCG group (p < 0.001 and p = 0.023, respectively, mixed effects negative binomial, Figure 3E). These data demonstrate that ΔLprG vaccination resulted in a striking reduction in both the establishment and dissemination of infection in this model.

Repeated 1 MID50 challenge infects most mice and shows greater stringency

In order to better model real-world dynamics including repeated exposure,[22,23] we designed studies incorporating repeated 1 MID50 challenge (Figure 4A). Two cohorts of C3HeB/FeJ mice (n = 18 mice per cohort, n = 36 total mice) were divided equally into three groups including naive, BCG, and ΔLprG. Each cohort was vaccinated at week 0, underwent four consecutive 1 MID50 H37Rv challenges at weeks 8, 9, 10, and 11, and at week 15, right and left lungs were dissected separately for bacterial load quantification. For a third cohort (n = 18 mice), lungs were fixed in formalin at week 15 for histopathological studies.

As expected, we observed an increased proportion of infected mice and a reduced proportion of mice with unilateral infection in the repeated challenge model (Figure 4B). Specifically, in the naive group, we observed that 11/12 (92%) of mice became infected, and only 1/11 (9%) mice demonstrated unilateral infection. Similar to single 1 MID50 challenge, there was a wide distribution of bacterial loads. In the naive group, repeated challenge also yielded increased average lung lobe bacterial loads relative to single low-dose challenge (5.69 $\log_{10}$ CFU vs. 4.90 $\log_{10}$ CFU, respectively, p = 0.002, Mann-Whitney U test). Histopathologic studies showed that repeated 1 MID50 challenge granulomas (up to 7 weeks post-initial challenge) in naive mice were indistinguishable in size and composition from those observed after 100 MID50 challenge (4 weeks post-challenge), consistent with early establishment of infection and prolonged bacterial replication (Figures S2 and S3A–S3C).

In the BCG group, we observed an infection rate of 12/12 (100%) including a unilateral infection rate of 2/12 (17%, Figure 4B). Thus, BCG vaccination did not reduce the rate of infection or increase the rate of unilateral infection (Figures 4C and 4D). In contrast, BCG showed a substantial 0.99 $\log_{10}$ reduction in lung lobe bacterial loads compared to the naive group (Figures 4B and 4E, p < 0.001, mixed effects negative binomial). In the ΔLprG group, we observed an infection rate of 9/9 (100%) including a unilateral infection rate of 4/19 (44%, Figure 4B). In contrast to single 1 MID50 challenge, following repeated challenge ΔLprG did not reduce infection rates relative to the naive and BCG groups (Figure 4C). However, we observed a trend
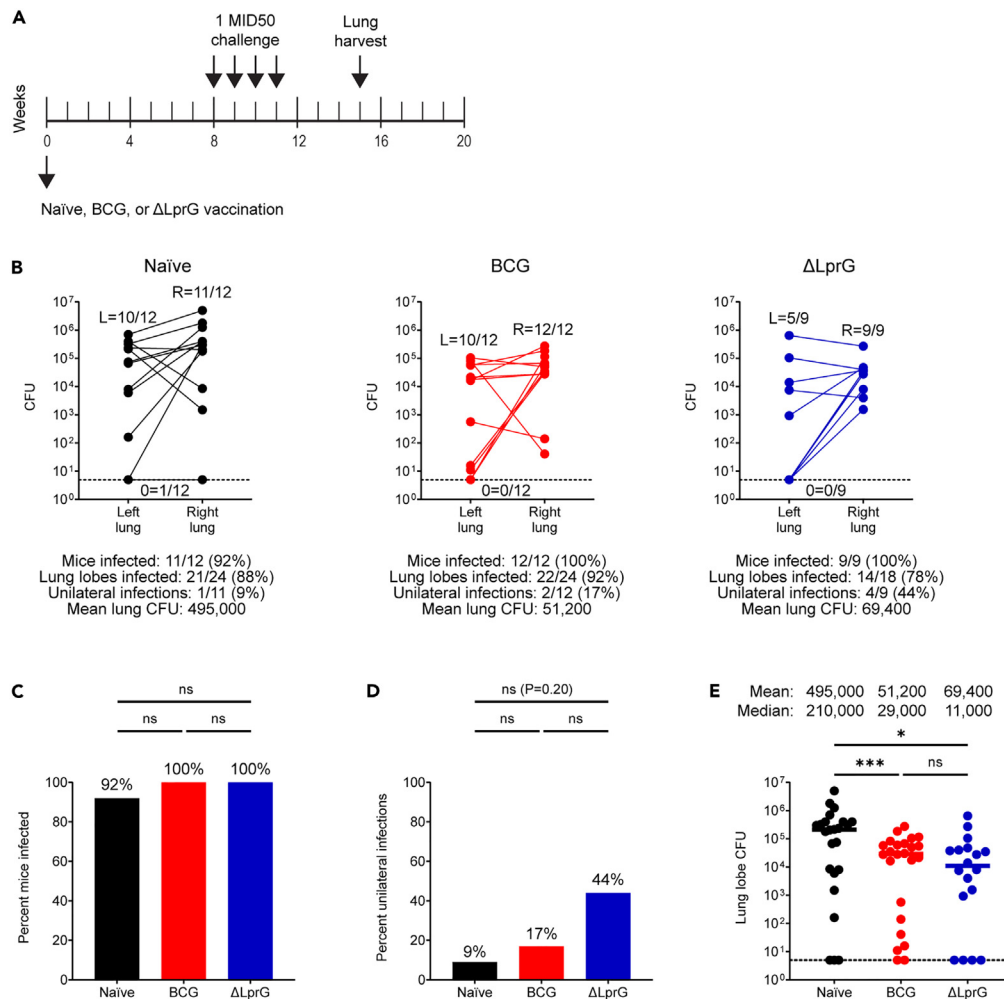
Figure 4. Vaccine protection with BCG and ΔLprG after repeated 1 MID50 H37Rv challenge in C3HeB/FeJ mice

(A) Study design (A).

(B) Two cohorts of C3HeB/FeJ mice (n = 18 mice per cohort, n = 36 mice total) were divided equally into naive, BCG, and ΔLprG groups. Vaccines were administered at week 0 followed by four weekly 1 MID50 H37Rv aerosol challenges between weeks 8–11 and right and left lung lobe harvesting at week 15 for lung lobe bacterial load quantification (B).

Bottom dotted line represents an LOD of 5 CFU. Histograms and dot plots summarizing data are shown in B (C–E). p values for infection rates between groups represent an exact logistic regression model (C and D). p values for bacterial loads between groups represent a mixed effects negative binomial model (E). For (E), bottom dotted line represents an LOD of 5 CFU and bars represent group medians. For all panels, * represents $p < 0.05$ and *** represents $p < 0.001$.

toward an increased proportion of mice with unilateral infection relative to the naive (44% vs. 11%) and BCG (44% vs. 17%) groups (Figure 4D). Finally, the ΔLprG group showed a 0.85 $\log_{10}$ reduction in average lung lobe bacterial loads relative to the naive group (Figures 4B and 4E, p = 0.016, mixed effects negative binomial model). Mice vaccinated with either BCG or ΔLprG had fewer and smaller granulomas than naive mice after repeated low-dose challenge, consistent with a delay in acquisition of disease or greater control of bacterial replication (Figure S3). Increased numbers of lymphocytes as well as increased perivascular lymphocytic cuffing were observed in granulomas from vaccinated mice.

Repeated 1 MID50 challenge facilitates correlates of protection analyses

We evaluated post-vaccination, pre-challenge serum cytokine levels among one cohort of repeated low-dose challenge mice in which all (6/6, 100%) naive animals became infected and compared them with post-challenge whole-lung CFU on a per-mouse basis. We observed that 7 of 35 assayed post-vaccination serum cytokines were negatively correlated with post-challenge bacterial loads (Figure 5). Notably, the
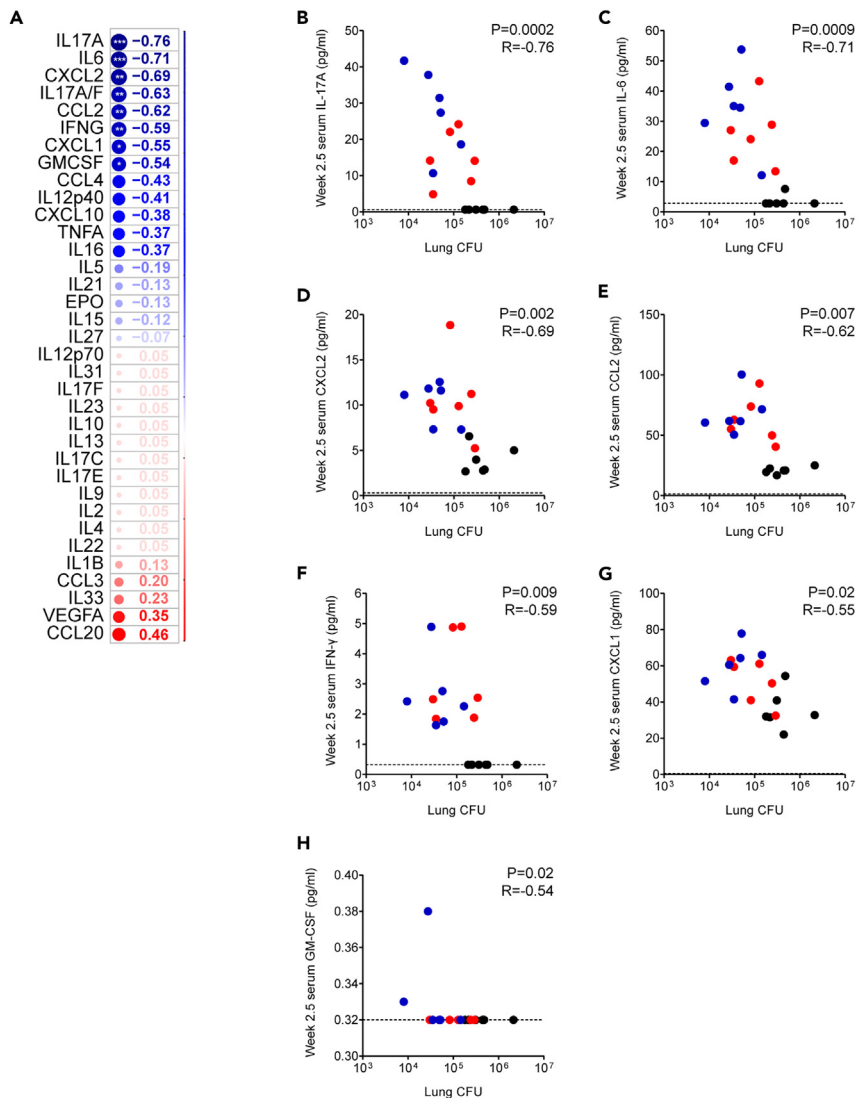
Figure 5. Pre-challenge serum cytokine levels correlated with bacterial loads among naive and BCG- and ΔLprG-vaccinated C3HeB/FeJ mice after four weekly 1 MID50 H37Rv challenges

(A–H) A cohort of C3HeB/FeJ mice (n = 18) was divided into naive (n = 6), BCG (n = 6), and ΔLprG (n = 6) groups. Vaccines were administered at week 0 and serum cytokines were measured at week 2.5. The cohort then underwent four weekly 1 MID50 H37Rv aerosol challenges between weeks 8–11 and right and left lung lobes harvested at week 15 for lung lobe bacterial load quantification. Two-tailed Spearman correlation coefficients comparing the serum expression levels of 35 cytokines measured at week 2.5 with whole-mouse bacterial loads measured at week 15 (A). * represents p < 0.05, ** represents p < 0.01, and *** represents p < 0.001. Individual two-tailed Spearman correlation plots for IL-17 (B), IL-6 (C), CXCL2 (D), CCL2 (E), IFN-γ (F), CXCL1 (G), and GM-CSF (H).

serum cytokine most correlated with reductions in bacterial load was IL-17A, a molecule that we and others have found to be correlated with protection in both mouse[5,24,25] and macaque[26] vaccine studies as well as natural infection studies in macaques[27] and humans.[28] Additional correlates included IL-6 and CXCL2 as we previously described in the 100 MID50 challenge model[5] as well as others including CCL2 and CXCL1 which to our knowledge have not previously been described as correlates of TB vaccine protection.

DISCUSSION

Preclinical TB vaccine studies have primarily relied on a 100 CFU murine aerosol challenge that does not model the low-dose dynamics that are thought to mediate transmission in humans. Moreover, BCG and

other preclinical vaccine candidates only show moderate reductions in bacterial loads, complicating the interpretation of vaccine protection in this model. In this study, we demonstrate striking protective efficacy of the live attenuated ΔLprG preclinical vaccine candidate against a low-dose challenge including prevention of detectable infection among a substantial subset of mice and anatomic containment to a single lung among all mice that are infected. These data provide an experimentally tractable model of substantive vaccine protection against TB and corroborate use of the low-dose model for preclinical vaccine development.

We show that ΔLprG reduces bacterial loads as well as two additional measures of vaccine protection that are not captured by the 100 CFU challenge model: prevention of detectable infection and prevention of dissemination to the contralateral lung. These data corroborate other recent work showing that BCG reduces detectable infection and disseminated infection in addition to traditional bacterial load measurements, although these studies required substantially larger numbers of mice due to the lower protective efficacy of BCG.[19,20] Therefore, the capacity of ΔLprG to abrogate detectable infection and disseminated infection with relatively small group sizes may provide an experimentally tractable model for assessing potent vaccines such as ΔLprG, including facilitating mechanistic studies evaluating immune molecules and subsets in mediating defined aspects of protection.

Mtb transmission typically occurs after repeated exposures, for example in the setting of infected household contacts.[22,23] Indeed, preclinical nonhuman primate (NHP) studies are increasingly performed with repeated low-dose Mtb challenge.[26] Similarly, repeated low-dose exposure is commonly used in the HIV field to test prophylactic interventions.[29,30] In both of these models, repeated challenge creates unique opportunities for measuring correlates of protection.[26,29,30] We therefore developed a repeated low-dose Mtb challenge model that resulted in increased challenge stringency and reduced vaccine efficacy compared with the single low-dose Mtb challenge model. Correlates of protection analysis suggested that serum IL-17A was a key correlate of vaccine protection as previously described[5,24,26] and identified additional biomarkers of protection including CCL2 and CXCL1 that to our knowledge have not previously been described in this context. The reduced capacity of ΔLprG to mediate prevention of detectable infection in the repeated challenge model may reflect a narrow protective window related to the limitations of murine immune responses to Mtb.[31]

Several aspects of vaccine protection mediated by ΔLprG in the low-dose model will be important to evaluate in future studies. We did not assess mice after four weeks, and data from later time points and survival studies could provide measures of longer term vaccine protection. Indeed, BCG provides long-term bacterial control in the low-dose model, in contrast to the short-lived protection observed after 100 CFU challenge.[20] Use of challenge strain barcoding[18,20] and analysis of spleen and other sites of dissemination like draining lymph nodes could provide a more granular understanding of vaccine protection. In addition, future studies could assess the contributions of myeloid and T cell subsets as well as the cytokines identified in our correlates analysis for their potential roles as regulators of ΔLprG vaccine protection in the low-dose model. Finally, intravenous administration of ΔLprG could be explored in the low-dose model, as recently reported for BCG in the 100 CFU mouse[32] and NHP[33] models.

In summary, we demonstrate that the attenuated TB vaccine candidate ΔLprG provides strikingly greater protection than BCG against low-dose challenge in mice, including prevention of detectable infection in the majority of animals and anatomic containment for all breakthrough infections. We further developed a repeated low-dose challenge model that was more stringent and identified biomarkers of vaccine protection. These data support a compelling framework for the preclinical evaluation of next-generation TB vaccine candidates that are more protective than BCG as well as studies dissecting the immunologic mechanisms that modulate Mtb infection and dissemination in addition to control of bacterial burden.

Limitations of the study

Our study of the protective efficacy of ΔLprG in the low-dose murine aerosol challenge has several limitations. First, our data are limited to the C3HeB/FeJ mouse and H37Rv challenge strains, and it will be important to show generalizability of our findings to additional mouse strains and heterologous challenge strains. Moreover, our necropsies were performed at four weeks and we did not perform longer term protection studies. In addition, we did not examine the status of dissemination to spleen. Finally, we did not perform immunophenotyping or mechanistic studies examining the roles of immune cells and pathways in mediating protection in the low-dose model.

STAR★METHODS

Detailed methods are provided in the online version of this paper and include the following:

- KEY RESOURCES TABLE
- RESOURCE AVAILABILITY
  - Lead contact
  - Material availability
  - Data and code availability
- EXPERIMENTAL MODEL AND STUDY PARTICIPANT DETAILS
  - Challenge and vaccine strains
  - Mouse strains, immunizations, and aerosol challenges
- METHOD DETAILS
  - PBMC flow cytometry
  - Serum cytokine analysis
  - Low dose challenge stock preparation and *in vivo* titration studies
  - Lung processing and CFU quantification
  - Histopathological studies
- QUANTIFICATION AND STATISTICAL ANALYSIS

SUPPLEMENTAL INFORMATION

Supplemental information can be found online at https://doi.org/10.1016/j.isci.2023.106963.

AUTHOR CONTRIBUTIONS

S.J.V., C.R.P., K.B.U., and D.H.B. conceptualized the study. S.J.V., D.S., J.Y., S.W., J.S., J.B., S.F.S., E.R.M., and X.L. performed in the mouse studies and immunology assays. M.A. led the bioinformatics. W.L. performed the statistics. A.J.M. performed the histopathology. S.J.V. and D.H.B. wrote the manuscript. All co-authors reviewed and edited the manuscript.

DECLARATION OF INTERESTS

A.J.M. and D.H.B. are co-inventors on a provisional vaccine patent PCT/US2020/059152 (Mycobacterial compositions and biomarkers for use in treatment and monitoring of therapeutic responsiveness).

REFERENCES

1. Global Tuberculosis Report (2021 (World Health Organization)). 2021.

2. Fine, P.E. (1995). Variation in protection by BCG: implications of and for heterologous immunity. Lancet *346*, 1339–1345. https://doi.org/10.1016/s0140-6736(95)92348-9.

3. Andersen, P., and Scriba, T.J. (2019). Moving tuberculosis vaccines from theory to practice. Nat. Rev. Immunol. *19*, 550–562. https://doi.org/10.1038/s41577-019-0174-z.

4. The End TB Strategy (2015 (World Health Organization), August 16, 2015.

5. Martinot, A.J., Blass, E., Yu, J., Aid, M., Mahrokhian, S.H., Cohen, S.B., Plumlee, C.R., Larocca, R.A., Siddiqi, N., Wakabayashi, S., et al. (2020). Protective efficacy of an attenuated Mtb ΔLprG vaccine in mice. PLoS Pathog. *16*, e1009096. https://doi.org/10.1371/journal.ppat.1009096.

6. Martinot, A.J., Farrow, M., Bai, L., Layre, E., Cheng, T.Y., Tsai, J.H., Iqbal, J., Annand, J.W., Sullivan, Z.A., Hussain, M.M., et al. (2016). Mycobacterial metabolic syndrome: LprG and Rv1410 regulate triacylglyceride levels, growth rate and virulence in *Mycobacterium tuberculosis*. PLoS Pathog. *12*, e1005351. https://doi.org/10.1371/journal.ppat.1005351.

7. Caruso, A.M., Serbina, N., Klein, E., Triebold, K., Bloom, B.R., and Flynn, J.L. (1999). Mice deficient in CD4 T cells have only transiently diminished levels of IFN-gamma, yet succumb to tuberculosis. J. Immunol. *162*, 5407–5416.

8. Flynn, J.L., Chan, J., Triebold, K.J., Dalton, D.K., Stewart, T.A., and Bloom, B.R. (1993). An essential role for interferon gamma in resistance to *Mycobacterium tuberculosis* infection. J. Exp. Med. *178*, 2249–2254. https://doi.org/10.1084/jem.178.6.2249.

9. Cooper, A.M., Dalton, D.K., Stewart, T.A., Griffin, J.P., Russell, D.G., and Orme, I.M. (1993). Disseminated tuberculosis in interferon gamma gene-disrupted mice. J. Exp. Med. *178*, 2243–2247. https://doi.org/10.1084/jem.178.6.2243.

10. Flynn, J.L., Goldstein, M.M., Chan, J., Triebold, K.J., Pfeffer, K., Lowenstein, C.J., Schreiber, R., Mak, T.W., and Bloom, B.R. (1995). Tumor necrosis factor-alpha is required in the protective immune response against Mycobacterium tuberculosis in mice. Immunity *2*, 561–572. https://doi.org/10.1016/1074-7613(95)90001-2.

11. Dillon, D.C., Alderson, M.R., Day, C.H., Lewinsohn, D.M., Coler, R., Bement, T., Campos-Neto, A., Skeiky, Y.A., Orme, I.M., Roberts, A., et al. (1999). Molecular characterization and human T-cell responses to a member of a novel Mycobacterium tuberculosis mtb39 gene family. Infect. Immun. *67*, 2941–2950. https://doi.org/10.1128/iai.67.6.2941-2950.1999.

12. Skeiky, Y.A.W., Alderson, M.R., Ovendale, P.J., Guderian, J.A., Brandt, L., Dillon, D.C., Campos-Neto, A., Lobet, Y., Dalemans, W., Orme, I.M., and Reed, S.G. (2004). Differential immune responses and protective efficacy induced by components of a tuberculosis polyprotein vaccine, Mtb72F, delivered as naked DNA or recombinant protein. J. Immunol. *172*, 7618–7628. https://doi.org/10.4049/jimmunol.172.12.7618.

13. Donald, P.R., Diacon, A.H., Lange, C., Demers, A.M., von Groote-Bidlingmaier, F., and Nardell, E. (2018). Droplets, dust and Guinea pigs: an historical review of tuberculosis transmission research, 1878-1940. Int. J. Tuberc. Lung Dis. *22*, 972–982. https://doi.org/10.5588/ijtld.18.0173.

14. Lin, P.L., Ford, C.B., Coleman, M.T., Myers, A.J., Gawande, R., Ioerger, T., Sacchettini, J., Fortune, S.M., and Flynn, J.L. (2014). Sterilization of granulomas is common in active and latent tuberculosis despite within-host variability in bacterial killing. Nat. Med. *20*, 75–79. https://doi.org/10.1038/nm.3412.

15. Ramakrishnan, L. (2012). Revisiting the role of the granuloma in tuberculosis. Nat. Rev. Immunol. *12*, 352–366. https://doi.org/10.1038/nri3211.

16. Cadena, A.M., Fortune, S.M., and Flynn, J.L. (2017). Heterogeneity in tuberculosis. Nat. Rev. Immunol. *17*, 691–702. https://doi.org/10.1038/nri.2017.69.

17. Cobelens, F., Suri, R.K., Helinski, M., Makanga, M., Weinberg, A.L., Schaffmeister, B., Deege, F., and Hatherill, M.; TB Vaccine Roadmap Stakeholder Group (2022). Accelerating research and development of new vaccines against tuberculosis: a global roadmap. Lancet Infect. Dis. *22*, e108–e120. https://doi.org/10.1016/s1473-3099(21)00810-0.

18. Plumlee, C.R., Duffy, F.J., Gern, B.H., Delahaye, J.L., Cohen, S.B., Stoltzfus, C.R., Rustad, T.R., Hansen, S.G., Axthelm, M.K., Picker, L.J., et al. (2021). Ultra-low dose aerosol infection of mice with Mycobacterium tuberculosis more closely models human tuberculosis. Cell Host Microbe *29*, 68–82.e5. https://doi.org/10.1016/j.chom.2020.10.003.

19. Plumlee, C.R., Duffy, F.J., Gern, B.H., Delahaye, J.L., Cohen, S.B., Rustad, T.R., Aitchison, J.D., Sherman, D.R., Zak, D.E., Gerner, M.Y., and Urdahl, K.B. (2020). Apparent sterilizing immunity in BCG-immunized mice challenged with an ultra-low dose of Mycobacterium tuberculosis. J. Immunol. *204*, 231.25. https://doi.org/10.4049/jimmunol.204.Supp.231.25.

20. Plumlee, C.R., Barrett, H.W., Shao, D.E., Lien, K.A., Cross, L.M., Cohen, S.B., Edlefsen, P.T., and Urdahl, K.B. (2023). Assessing vaccine-mediated protection in an ultra-low dose Mycobacterium tuberculosis murine model. bioRxiv. Preprint at. https://doi.org/10.1101/2023.03.22.533820.

21. Kramnik, I., Dietrich, W.F., Demant, P., and Bloom, B.R. (2000). Genetic control of resistance to experimental infection with virulent Mycobacterium tuberculosis. Proc. Natl. Acad. Sci. USA *97*, 8560–8565. https://doi.org/10.1073/pnas.150227197.

22. Migliori, G.B., Nardell, E., Yedilbayev, A., D'Ambrosio, L., Centis, R., Tadolini, M., van den Boom, M., Ehsani, S., Sotgiu, G., and Dara, M. (2019). Reducing tuberculosis transmission: a consensus document from the world health organization regional office for Europe. Eur. Respir. J. *53*, 1900391. https://doi.org/10.1183/13993003.00391-2019.

23. Churchyard, G., Kim, P., Shah, N.S., Rustomjee, R., Gandhi, N., Mathema, B., Dowdy, D., Kasmar, A., and Cardenas, V. (2017). What we know about tuberculosis transmission: an overview. J. Infect. Dis. *216*, 629–635. https://doi.org/10.1093/infdis/jix362.

24. Khader, S.A., Bell, G.K., Pearl, J.E., Fountain, J.J., Rangel-Moreno, J., Cilley, G.E., Shen, F., Eaton, S.M., Gaffen, S.L., Swain, S.L., et al. (2007). IL-23 and IL-17 in the establishment of protective pulmonary CD4+ T cell responses after vaccination and during Mycobacterium tuberculosis challenge. Nat. Immunol. *8*, 369–377. https://doi.org/10.1038/ni1449.

25. Woodworth, J.S., Clemmensen, H.S., Battey, H., Dijkman, K., Lindenstrøm, T., Laureano, R.S., Taplitz, R., Morgan, J., Aagaard, C., Rosenkrands, I., et al. (2021). A Mycobacterium tuberculosis-specific subunit vaccine that provides synergistic immunity upon co-administration with Bacillus Calmette-Guérin. Nat. Commun. *12*, 6658. https://doi.org/10.1038/s41467-021-26934-0.

26. Dijkman, K., Sombroek, C.C., Vervenne, R.A.W., Hofman, S.O., Boot, C., Remarque, E.J., Kocken, C.H.M., Ottenhoff, T.H.M., Kondova, I., Khayum, M.A., et al. (2019). Prevention of tuberculosis infection and disease by local BCG in repeatedly exposed rhesus macaques. Nat. Med. *25*, 255–262. https://doi.org/10.1038/s41591-018-0319-9.

27. Gideon, H.P., Hughes, T.K., Tzouanas, C.N., Wadsworth, M.H., 2nd, Tu, A.A., Gierahn, T.M., Peters, J.M., Hopkins, F.F., Wei, J.R., Kummerlowe, C., et al. (2022). Multimodal profiling of lung granulomas in macaques reveals cellular correlates of tuberculosis control. Immunity *55*, 827–846.e10. https://doi.org/10.1016/j.immuni.2022.04.004.

28. Nathan, A., Beynor, J.I., Baglaenko, Y., Suliman, S., Ishigaki, K., Asgari, S., Huang, C.C., Luo, Y., Zhang, Z., Lopez, K., et al. (2021). Multimodally profiling memory T cells from a tuberculosis cohort identifies cell state associations with demographics, environment and disease. Nat. Immunol. *22*, 781–793. https://doi.org/10.1038/s41590-021-00933-1.

29. Andrews, C.D., Spreen, W.R., Mohri, H., Moss, L., Ford, S., Gettie, A., Russell-Lodrigue, K., Bohm, R.P., Cheng-Mayer, C., Hong, Z., et al. (2014). Long-acting integrase inhibitor protects macaques from intrarectal simian/human immunodeficiency virus. Science *343*, 1151–1154. https://doi.org/10.1126/science.1248707.

30. Vidal, S.J., Bekerman, E., Hansen, D., Lu, B., Wang, K., Mwangi, J., Rowe, W., Campigotto, F., Zheng, J., Kato, D., et al. (2022). Long-acting capsid inhibitor protects macaques from repeat SHIV challenges. Nature *601*, 612–616. https://doi.org/10.1038/s41586-021-04279-4.

31. Bloom, B.R., and Modlin, R.L. (2016). Mechanisms of defense against intracellular pathogens mediated by human macrophages. Microbiol. Spectr. *4*. https://doi.org/10.1128/microbiolspec.MCHD-0006-2015.

32. Kaufmann, E., Sanz, J., Dunn, J.L., Khan, N., Mendonça, L.E., Pacis, A., Tzelepis, F., Pernet, E., Dumaine, A., Grenier, J.C., et al. (2018). BCG educates hematopoietic stem cells to generate protective innate immunity against. Cell *172*, 176–190.e19. https://doi.org/10.1016/j.cell.2017.12.031.

33. Darrah, P.A., Zeppa, J.J., Maiello, P., Hackney, J.A., Wadsworth, M.H., 2nd, Hughes, T.K., Pokkali, S., Swanson, P.A., 2nd, Grant, N.L., Rodgers, M.A., et al. (2020). Prevention of tuberculosis in macaques after intravenous BCG immunization. Nature *577*, 95–102. https://doi.org/10.1038/s41586-019-1817-8.

STAR★METHODS

KEY RESOURCES TABLE

REAGENT or RESOURCE	SOURCE	IDENTIFIER
Antibodies		
Rat anti-mouse CD3	BD Biosciences	Cat# 612803; RRID: AB_2870130
Rat anti-mouse CD19	BioLegend	Cat# 115540; RRID: AB_2563067
Rat anti-mouse CD4	BioLegend	Cat# 100566; RRID: AB_2563685
Rat anti-mouse CD8a	BD Biosciences	Cat# 563786; RRID: AB_2732919
Rat anti-mouse CD44	BD Biosciences	Cat# 563971; RRID: AB_2738518
Rat anti-mouse CD62L	BioLegend	Cat# 104420; RRID: AB_493376
Rat anti-mouse IFN-γ	BioLegend	Cat# 505830; RRID: AB_2563105
Rat anti-mouse IL-2	BioLegend	Cat# 503808; RRID: AB_315302
Rat anti-mouse TNF-α	BioLegend	Cat# 506338; RRID: AB_2562918
Rat anti-mouse IL-17A	BioLegend	Cat# 506922; RRID: AB_2125010
Rat anti-mouse IL-4	BD Biosciences	Cat# 554436; RRID: AB_398556
Bacterial and virus strains		
H37Rv	Rubin laboratory	N/A
BCG Pasteur	Urdahl laboratory	N/A
Chemicals, peptides, and recombinant proteins		
Purified protein derivative (PPD)	CedarLane	2390(SS)
Critical commercial assays		
U-PLEX Biomarker Group 1 (ms) 35-Plex kit	Meso Scale Discovery	K15083K
Experimental models: Organisms/strains		
C3HeB/FeJ mice	Jackson Laboratory	000658
Software and algorithms		
FloJo 10.8.1	BD Biosciences	https://www.bdbiosciences.com/en-us/products/software
Discovery Workbench 4.0	Meso Scale Discovery	https://www.mesoscale.com/en/products_and_services/software
GraphPad Prism 9.4.0	GraphPad	https://www.graphpad.com/features
R and R studio	Open source	https://www.r-project.org/

RESOURCE AVAILABILITY

Lead contact

Further information and requests for resources and reagents should be directed to and will be fulfilled by the lead contact, Dan H. Barouch (dbarouch@bidmc.harvard.edu).

Material availability

This study did not generate new materials.

Data and code availability

- Data reported in this paper will be shared by the lead contact upon request.

- This paper does not report original code.

- Any additional information required to reanalyze the data reported in this paper is available from the lead contact upon request.

EXPERIMENTAL MODEL AND STUDY PARTICIPANT DETAILS

Challenge and vaccine strains

H37Rv challenge strain was obtained from the Rubin laboratory (Harvard School of Public Health). BCG vaccine strain was obtained from the Urdahl laboratory (University of Washington). ΔLprG vaccine strain was generated in our laboratory as previously described.[5] All challenge and vaccine strains were grown in media consisting of Middlebrook 7H9 (BD Difco) containing 10% Middlebrook OADC (BD BBL), 0.5% glycerol (Sigma Aldrich), and 0.05% tween 80 (Sigma Aldrich). For preparation of vaccine stocks, vaccine strains were grown in complete growth medium as above additionally supplemented with 0.05% tyloxapol (Sigma Aldrich). Cells were pelleted twice with resuspension in PBS containing 0.05% tyloxapol and then pelleted a third time with resuspension in PBS containing 0.05% tyloxapol and 15% glycerol. Next cells were passaged though a 40 μm filter and then a 20 μm filter for clump removal, followed by storage at −80°C and titering by agar outgrowth assay. For low dose challenge studies, H37Rv culture was grown to an optical density (OD) of 1 followed by passaging through a 5 μm filter to generate a single-cell suspension, resulting in an approximately 2-$\log_{10}$ reduction in titer as measured by agar outgrowth assay.

Mouse strains, immunizations, and aerosol challenges

6-8 old female C3HeB/FeJ mice were obtained from Jackson Laboratory (strain 000658) and stored in sterile conditions at the Harvard School of Public Health. All mouse procedures were performed in accordance with Institutional Animal Care and Use Committee (IACUC) guidelines. All immunizations were performed SC in 8 week-old female mice. 1×10^6 CFU of tittered vaccine strain was used for all challenge studies. 100 μL of optical density (OD) 1 vaccine strain culture was used for the immunogenicity study. For 50–100 CFU challenge, a Glas-Col instrument was used and challenge stocks were titrated to result in a day 1 lung bacterial load of approximately 50–100 CFU. For low dose challenge, the same instrument was used and singe-cell suspension challenge stocks were titrated to result in a week 4 infection rate of approximately 60–70% in accordance with the Poisson distribution.

METHOD DETAILS

PBMC flow cytometry

For immunological studies mice were bled via the submandibular route into RPMI (Gibco) containing 5% EDTA (Invitrogen) route in accordance with IACUC guidance. Buffy layer containing PBMC were isolated via Ficoll (GE Healthcare) centrifugation and transferred into RPMI supplemented with 10% FBS (Gibco) and 1% penicillin-streptomycin (Fisher Scientific). Cells were stimulated with PPD (Cedarlane) at 400 ng of peptide per test or media control for 1 h followed by GolgiStop/GolgiPlug (BD Biosciences) overlay for 6 h at 37°C and then rested overnight 4°C. PBMCs were then stained with live/dead and cell surface markers in MACS solution (Miltenyi) supplemented with 2% BSA (Miltenyi) prior to permeabilization with Cytofix/Cytoperm (BD Biosciences) and staining with intracellular markers in Perm/Wash (BD Biosciences). PBMCs were then fixed in 2% formaldehyde and stored at 4°C until flow cytometry on an LSR II flow cytometer (BD Biosciences). Cell surface markers included CD3 (clone 17A2, BD Biosciences), CD19 (clone 6D5, BioLegend), CD4 (clone RM4-5, BioLegend), CD8a (clone 53-6.7, BD Biosciences), CD44 (clone IM7, BD Biosciences), and CD62L (clone MEL-14, BioLegend). Intracellular markers included IFN-γ (clone XMG1.2, BioLegend), IL-2 (clone JES6-5H4, BioLegend), TNF-α (clone MP6-XT22, BioLegend), IL17-A (clone TC11-18H10.1, BioLegend), and IL-4 (clone 11B11, BD Biosciences). Data were analyzed using FloJo 10.8.1 software.

Serum cytokine analysis

Plasma levels of 35 biomarkers were tested using U-PLEX Biomarker Group 1 (ms) 35-Plex kits from Meso Scale Discovery (MSD, Rockville, MD). The 35 biomarkers and their detection limits (LLODs) are EPO (4.5 pg/mL), GM-CSF (0.16 pg/mL), IFN-γ (0.16 pg/mL), IL-12p70 (48 pg/mL), IL-1β (3.1 pg/mL), IL-2 (1.1 pg/mL), IL-5 (0.63 pg/mL), IL-6 (4.8 pg/mL), KC/GRO (4.8 pg/mL), TNF-α (1.3 pg/mL), IL-10 (3.8 pg/mL), IL-13 (2.7 pg/mL), IL-15 (24 pg/mL), IL-17F (24 pg/mL), IL-23 (4.9 pg/mL), IL-27p28/IL-30 (8.7 pg/mL), IL-31 (45 pg/mL), IL-33 (2.2 pg/mL), IL-4 (0.56 pg/mL), VEGF-A (0.77 pg/mL), IL-12/IL-23p40 (1.4 pg/mL), IL-16 (3.6 pg/mL), IL-17A (0.30 pg/mL), IL-17C (2.3 pg/mL), IL-17E/IL-25 (1.6 pg/mL), IL-21 (6.5 pg/mL), IL-22 (1.2 pg/mL), IL-17A/F (0.61 pg/mL), IL-9 (1.4 pg/mL), IP-10 (0.51 pg/mL), MCP-1 (1.4 pg/mL), MIP-1α (0.21 pg/mL), MIP-1β (13 pg/mL), MIP-2 (0.30 pg/mL), MIP-3α (0.10 pg/mL). All above assays were done by Metabolism and Mitochondrial Research Core (Beth Israel Deaconess Medical Center, Boston, MA) following

manufacturer's instruction. The assay plates were read by MESO QUICKPLEX SQ 120 instrument and data were analyzed by Discovery Workbench 4.0 software.

Low dose challenge stock preparation and *in vivo* titration studies

H37Rv challenge strain was obtained and propagated as detailed above. Low dose challenge stock was generated as previously described.[18] Briefly, H37Rv was grown to an OD of 0.7–0.8. Cultures were passed through a 5 μm filter in order to generate a single cell suspension prior to aliquoting, freezing at −80°C, and tittering. For *in vivo* titration, challenges were performed as detailed above. We first estimated a 100-fold reduction in challenge dose relative to 50–100 CFU challenge and challenged mice with three $\log_{10}$ dilutions centered around the predicted low dose challenge dose. This identified a challenge dose with a 44% infection rate and was followed by a secondary dose titration study with three $\log_2$ dilutions centered around the predicted low dose challenge dose.

Lung processing and CFU quantification

Mice were euthanized 4 weeks following single 50–100 CFU challenge, 4 weeks following single low dose challenge, or 4 weeks following the final weekly low dose challenge in the repeated low dose challenge model. For 50–100 CFU challenge, both lung lobes were dissected *en bloc* whereas for low dose challenge right and left lung lobes were dissected separately. Tissues were placed into gentleMACS M Tubes (Miltenyi Biotec 130-096-335) containing 5 mL of PBS and mechanically dissociated using a gentleMACS Dissociator (Miltenyi Biotec). Lysates were then plated in serial $\log_{10}$ dilutions onto 100 × 15mm Middlebrook 7H10 plates (Hardy Diagnosatics). In order to achieve an LOD of 5 CFU in low dose challenge studies, we additionally plated 1 mL of lysate onto to two 150 × 15mm plates containing Middlebrook 7H10 agar (BD Difco), 10% Middlebrook OADC (BD BBL), 0.5% glycerol (Sigma Aldrich), and cycloheximide (Sigma Aldrich) at 100 μg/mL. CFU were counted after a 3 weeks incubation at 37°C.

Histopathological studies

Lungs were insufflated with 10% neutral buffer formalin for 48 h then transferred to 70% ethanol and processed routinely into paraffin blocks for hematoxylin and eosin or Ziehl-Neelsen acid-fast staining. Whole slide scanning (20x) was performed using a Midi II Pannoramic scanner (Epredia) and images evaluated by a boarded veterinary pathologist (AJM) using HALO (Indicalabs). Immune subsets including lymphocytes and macrophages were identified by hematoxylin and eosin staining by a board-certified veterinary pathologist (AJM) based on morphology.

QUANTIFICATION AND STATISTICAL ANALYSIS

Pairwise tests on immunogenicity and 50–100 CFU challenge data were performed using GraphPad Prism 9.4.0 software. Heatmaps were generated using the R package pheatmap. Cytokines plasma levels were normalized using the Z score method implemented in the pheatmap package. The correlation of cytokines with lung CFU was performed using the R package corrplot and Spearman's method. Statistical evaluation was assessed using a t-test distribution implemented in the R cor.test function. Rates of animal level infection (any lobe vs. none) were compared using exact logistic regression models. The composite infection outcomes (none vs. one lobe vs. both lobes) were analyzed using ordinal logistic regression models under the assumption of proportional odds. Between-group differences in bacterial loads were analyzed using mixed effects negative binomial regression models while controlling for lobe side/size (right vs. left). Two lobes of the same animal were considered a cluster, and animals were considered independent from each other.